



The crystal structures of benzylammonium phenylacetate and its hydrate

David Hess^{a*} and Peter Mayer^b^aInstitut Laue-Langevin, 71 Avenue des Martyrs, 38000 Grenoble, France, and ^bLudwig-Maximilians-Universität, Department Chemie, Butenandtstrasse, 5–13, 81377 München, Germany. *Correspondence e-mail: hessd@ill.fr

Received 11 December 2018

Accepted 7 January 2019

Edited by L. Van Meervelt, Katholieke Universiteit Leuven, Belgium

Keywords: crystal structure; hydrogen bonding; Hirshfeld analysis; intermolecular interactions; ammonium carboxylate salts.**CCDC references:** 1889253; 1889252**Supporting information:** this article has supporting information at journals.iucr.org/e

The title compounds benzylammonium phenylacetate, $C_7H_{10}N^+ \cdot C_8H_7O_2^-$ (**1**), and its monohydrate, $C_7H_{10}N^+ \cdot C_8H_7O_2^- \cdot H_2O$ (**2**), can be obtained by evaporating methanolic solutions containing equimolar amounts of benzylamine and phenylacetic acid in the absence and presence of water, respectively. N—H···O hydrogen bonds in the crystal structure of **1** lead to the formation of hydrophilic channels running along the *b*-axis direction. The hydrogen-bonding system is best described by fused $R_4^3(10)$ ring patterns, often observed in ammonium carboxylate salts. In **2**, the presence of the crystal water leads to the formation of a two-dimensional hydrogen-bonding network. The benzyl moieties in **1** and **2** form hydrophobic layers in the crystal structures with the aromatic rings adopting edge-to-face arrangements.

1. Chemical context

Many proteins can self-assemble into insoluble aggregates, so-called amyloids, with a high content of β -strands. Amyloid fibrils are qualitatively similar for different proteins, with filaments of a few nanometers in diameter that can grow up to several micrometers in length (McManus *et al.*, 2016). The amyloid state of proteins is linked to various human diseases, *e.g.* Alzheimer's disease (Eisenberg & Jucker, 2012). Besides proteins, oligopeptides (Ozbas *et al.*, 2004) down to simple dipeptides (Reches & Gazit, 2003) and even the amino acid phenylalanine (Mossou *et al.*, 2014; Do *et al.*, 2015) can also self-assemble into stable nanofilaments in aqueous solution. Apart from the obvious link to amyloid diseases, such structures are also interesting for technical applications (Gazit, 2007; Manna *et al.*, 2015). Hydrogen bonds between ammonium and carboxylate groups, as well as the presence of hydrophobic residues (*e.g.* aromatic residues) play an important role in the formation of self-assembled structures of (di)peptides or amino acids (Görbitz, 2010; Mossou *et al.*, 2014; Reches & Gazit, 2003). Similarly, the packing motifs of ammonium carboxylate salts are governed by the formation of hydrogen-bonded networks between the ammonium and carboxylate residues (Kinbara *et al.*, 1996; Odendal *et al.*, 2010).

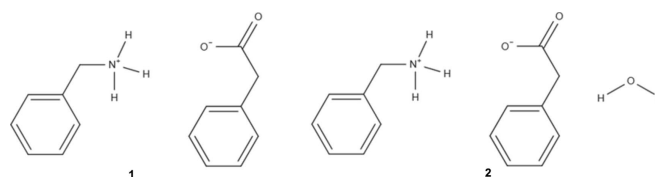
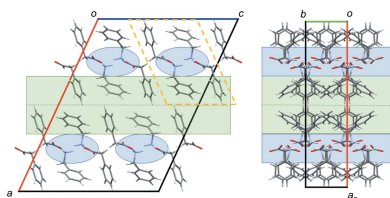


Table 1

 Contributions of close intermolecular contacts to the Hirshfeld surface areas of the molecules in **1** and **2**.

Compound	molecule	O...H	H...O	C...H	H...C	C...O	O...C	H...H
1	benzylammonium	0.0	15.8	13.6	13.8	1.3	0.0	55.5
	phenylacetate	21.5	4.1	16.9	6.6	0.0	0.7	50.2
2	benzylammonium	0.0	13.2	15.6	11.4	0.0	0.0	59.7
	phenylacetate	21.6	5.2	15.7	11.3	0.3	0.2	45.7
	water	30.5	22.4	0.0	1.8	0.0	0.0	44.9

Herein, we report the crystal structures of benzylammonium phenylacetate and its hydrate. Both show a similar crystal packing to the zwitterionic form of L-phenylalanine reported by Mossou *et al.* (2014). This resemblance raises the question of whether a system such as benzylammonium phenylacetate is also capable of forming nanofilaments.

2. Structural commentary

Benzylammonium phenylacetate (**1**) crystallizes in the monoclinic space group $C2/c$ and its hydrate (**2**) in the monoclinic space group $P2_1/n$. The asymmetric units of **1** and its hydrate **2** are shown in Fig. 1. In compound **1**, the ammonium group of the benzylammonium is orientated almost perpendicular to the phenyl ring [$90.2(2)^\circ$], while the carboxylate group of the phenylacetate adopts a torsion angle of $-70.2(4)^\circ$, while in the hydrate **2** the torsion angles between the phenyl rings and the functional groups are $72.4(4)$ and $54.4(4)^\circ$ for the phenylacetate and benzylammonium, respectively.

3. Supramolecular features

3.1. Crystal packing

The crystal packing of benzylammonium phenylacetate (**1**) consists of columns arranged around the twofold screw axis along b (Fig. 2). These columns are composed of hydrophilic channels, formed by the ammonium and carboxylate groups, surrounded by a shell made up by the phenyl moieties. The crystal packing of the hydrate (**2**) consists of hydrophilic and hydrophobic layers alternating along the c -axis direction, as shown in Fig. 3. The hydrophilic layer is composed of the water molecules, the ammonium and the carboxylate groups.

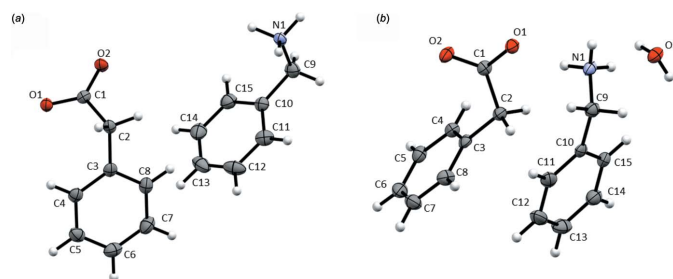


Figure 1
ORTEP representation of the asymmetric unit in (a) **1** and (b) **2** (50% probability ellipsoids).

3.2. Intermolecular contacts and Hirshfeld analysis

We used *CrystalExplorer17* to analyse the Hirshfeld surfaces of the molecules in the crystal structures of **1** and **2** and to quantify intermolecular contacts between them (Turner *et al.*, 2017; McKinnon *et al.*, 2007). Table 1 summarizes the relative contributions to the Hirshfeld surface areas for the intermolecular contacts found in the molecules of **1** and **2**.

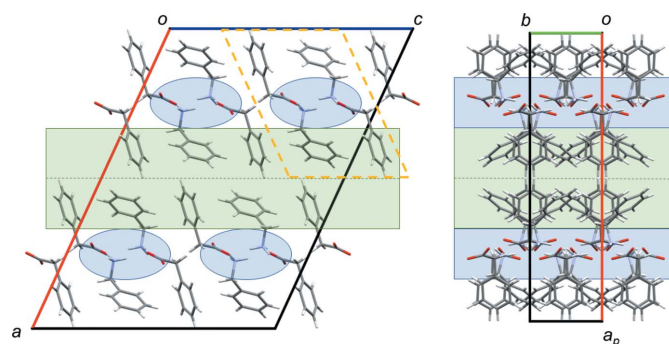


Figure 2
Crystal packing of **1** with views along the b axis (left) and along the c axis (right). Yellow dotted lines mark a column arranged around a twofold screw axis. Hydrophilic areas are highlighted in blue, hydrophobic areas in green.

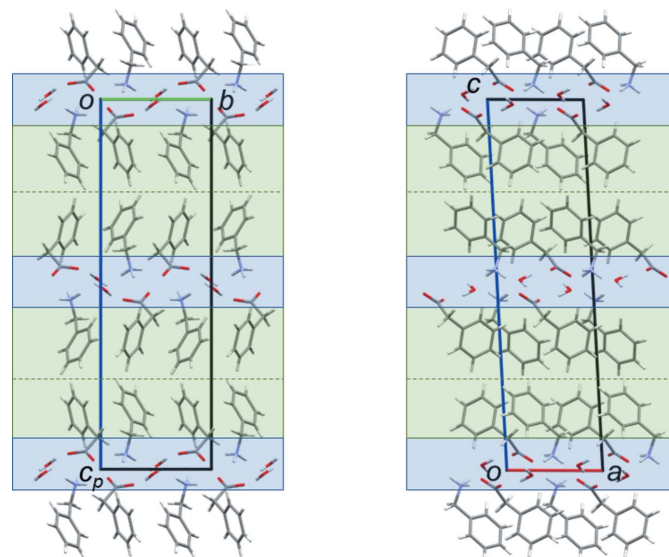


Figure 3
Crystal packing of **2** with views along the a axis (left) and along the b axis (right). Hydrophilic areas are highlighted in blue, hydrophobic areas in green.

There are three main groups of (inner···outer) intermolecular contacts that can be found on the Hirshfeld surfaces, namely O···H/H···O, C···H/H···C and H···H intermolecular contacts. Fig. 4 shows the fingerprint plots of the benzylammonium and phenylacetate molecules in **1** and **2**, highlighting the O···H/H···O and C···H/H···C contacts.

Mapping the Hirshfeld surfaces with different functions is a helpful tool for visualizing the nature of those intermolecular contacts. For example, the normalized contact distance d_{norm} mapped on the Hirshfeld surface using a red–white–blue colour scheme indicates distances shorter, around or greater than the van der Waals separation distances, respectively. The normalized contact distance is defined by the following equation

$$d_{norm} = \frac{d_i - r_i^{vdw}}{r_i^{vdw}} + \frac{d_e - r_e^{vdw}}{r_e^{vdw}},$$

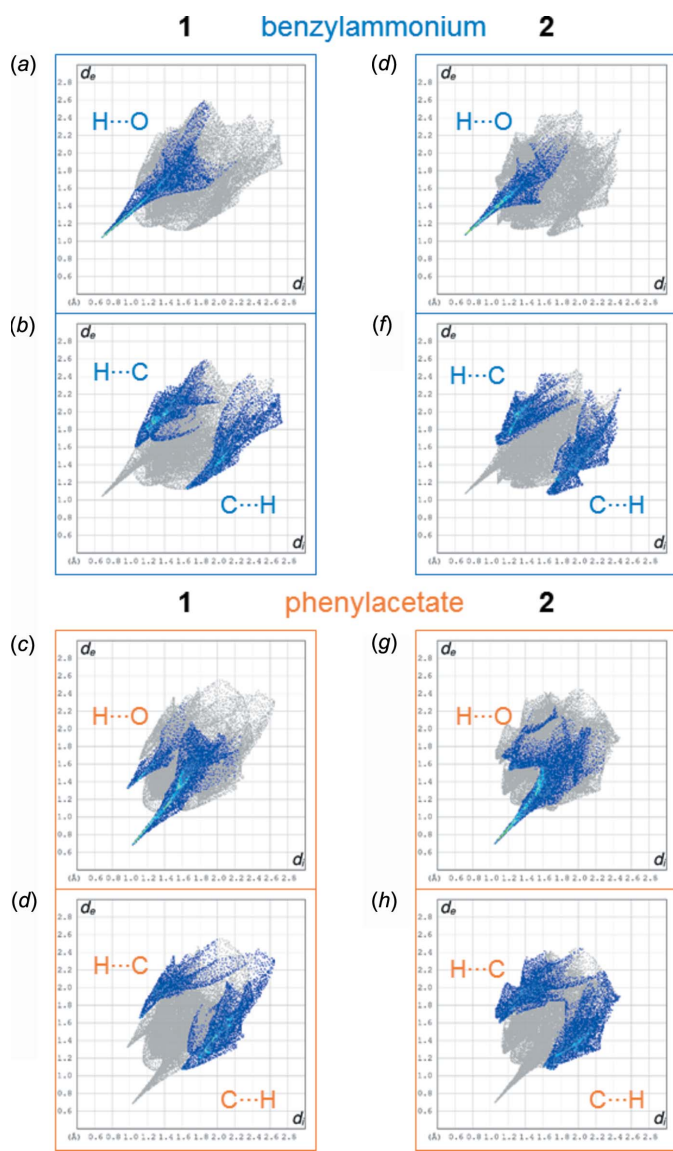


Figure 4
Comparison of the fingerprint plots of the benzylammonium and phenylacetate molecules in **1** and **2**, highlighting O···H/H···O and C···H/H···C contacts. d_i and d_e are plotted in Å on the x- and y-axis, respectively.

where d_i and d_e are the distances to the nearest atoms inside and outside the surface and r^{vdw} is the van der Waals radius of the appropriate atom internal or external to the surface (McKinnon *et al.*, 2007). Fig. 5 shows the benzylammonium and phenylacetate molecules in **1** with d_{norm} mapped. A number of contacts with distances below the sum of the van der Waals radius can directly be identified by red spots. The most intense ones (A/A' , B/B' , C/C' in Fig. 5) can be attributed to N–H···O hydrogen bonds between the benzylammonium and phenylacetate molecules. The remaining spots are due to non-classical C–H···O hydrogen bonds among the phenylacetate molecules (D/D' , E/E' in Fig. 5) and an aliphatic C–H··· π interaction between benzylammonium and phenylacetate (F/F' in Fig. 5). Fig. 6 shows the normalized contact distance d_{norm} mapped on the Hirshfeld surface of the molecules in **2**, highlighting the N–H···O (C/C' , D/D' and E/E') and O–H···O (A/A' , B/B') hydrogen bonds as the primary intermolecular interactions, followed by the non-classical C–H···O hydrogen bonds (F/F' and G/G'). Two further close contacts of the type C–H···C (H/H' and I/I') can be identified.

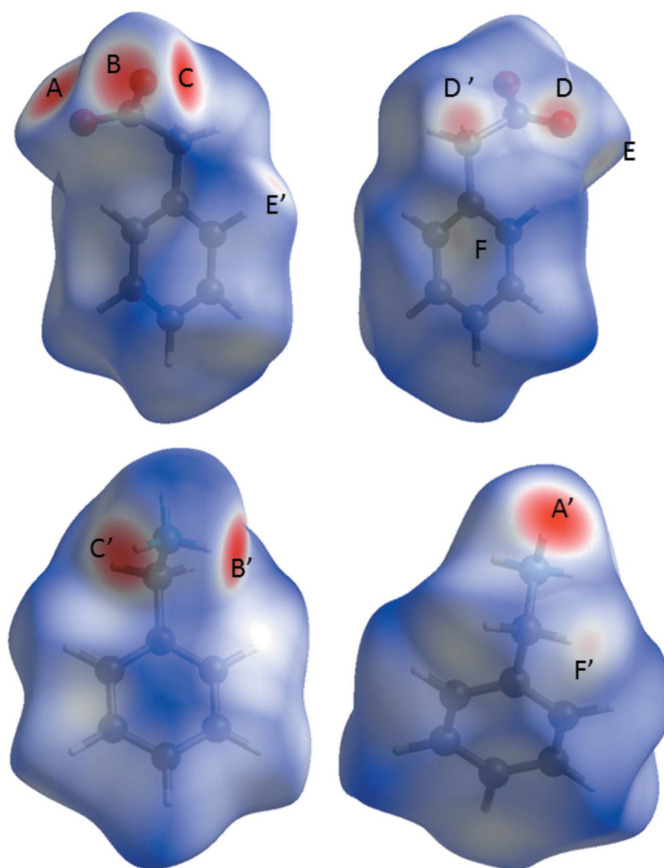
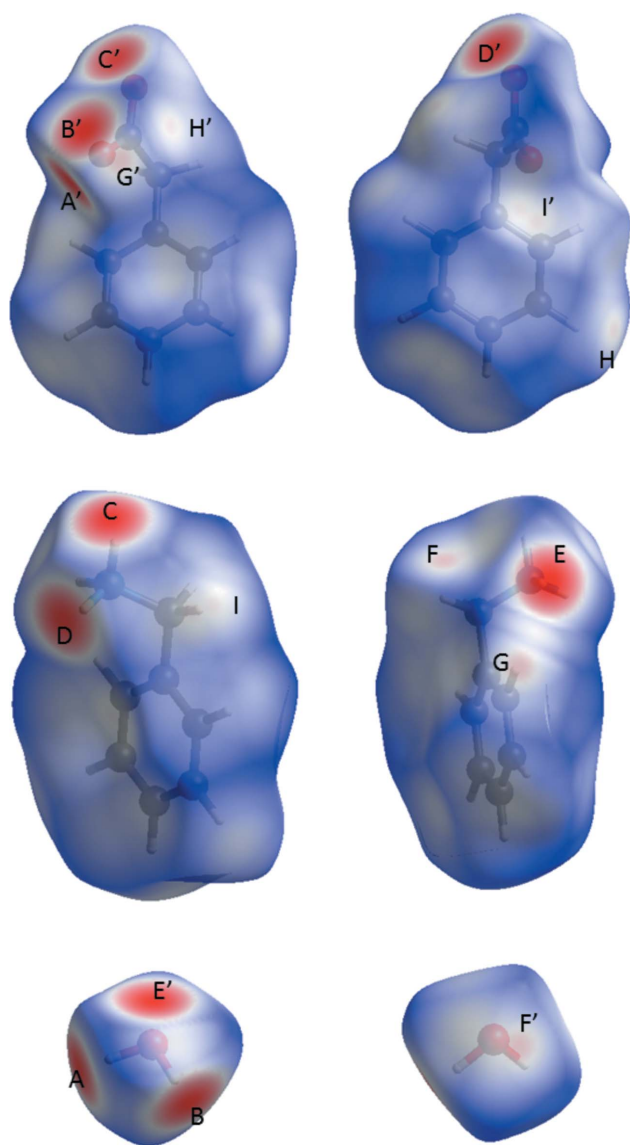


Figure 5
Hirshfeld surfaces of benzylammonium (bottom) and phenylacetate (top) molecules in **1** mapped with d_{norm} . Red spots indicate contact areas shorter than the van der Waals separation. Those contacts can be attributed to the following intermolecular interactions: N1–H11···O1 (A/A'), N–H13···O2 (B/B'), N–H12···O2 (C/C'), C2–H2B···O1 (D/D'), C8–H8···O1 (E/E'), and C9–H9B··· π (F/F'). The map ranges from –0.6825 to 1.3335 a.u. for phenylacetate and –0.6822 to 1.4269 a.u. for benzylammonium.


Figure 6

Hirshfeld surfaces of phenylacetate (top), benzylammonium (middle) and water (bottom) molecules in **2** mapped with d_{norm} . Red spots indicate contact areas shorter than the van der Waals separation. Contacts can be attributed to the following intermolecular interactions: O3—H32...O2 (*A/A'*), O3—H31...O2 (*B/B'*), N—H12...O1 (*C/C'*), N—H11...O1 (*D/D'*), N—H13...O3 (*E/E'*), C9—H9B...O3 (*F/F'*), C15—H15...O2 (*G/G'*), C5—H5...C1 (*H/H'*) and C9—H9A...C4 (*I/I'*). The map ranges from -0.6666 to 1.2024 a.u. for phenylacetate, -0.6268 to 1.1600 a.u. for benzylammonium and -0.6680 to 1.0780 a.u. for water.

Fig. 4 shows the fingerprint plots of the benzylammonium and phenylacetate molecules in **1** and **2**. O...H/H...O contacts can be attributed mainly to classical and non-classical, *i.e.* C—H...O, hydrogen bonds. Naturally no O...H contacts, but only H...O contacts are found on the Hirshfeld surface of the benzylammonium molecules, resulting in a single spike (*i.e.* N—H...O hydrogen bonds) highlighted in the fingerprint plots (*a*) and (*e*) in Fig. 4. The phenylacetate molecules can act as hydrogen-bond acceptors *via* their oxygen atoms (*i.e.* O...H contacts), visible through the intense spike in the fingerprint plots (*c*) and (*d*) in Fig. 4. In addition, H...O

Table 2

 Hydrogen-bond geometry (Å, °) for **1**.

Cg1 is the centroid of the C3—C8 ring.

<i>D</i> —H... <i>A</i>	<i>D</i> —H	H... <i>A</i>	<i>D</i> ... <i>A</i>	<i>D</i> —H... <i>A</i>
N1—H11...O1 ⁱ	0.97 (2)	1.77 (2)	2.7177 (19)	165 (2)
N1—H12...O2 ⁱⁱ	1.01 (2)	1.73 (2)	2.7306 (19)	170.1 (18)
N1—H13...O2 ⁱⁱⁱ	0.95 (3)	1.85 (3)	2.7938 (19)	174 (2)
C2—H2B...O1 ^{iv}	0.99	2.40	3.375 (2)	169
C8—H8...O1 ⁱⁱⁱ	0.95	2.63	3.539 (2)	161
C9—H9...Cg1 ^v	0.95	2.92	3.877 (2)	163

Symmetry codes: (i) $-x + \frac{1}{2}, y + \frac{3}{2}, -z + \frac{1}{2}$; (ii) $-x + \frac{1}{2}, y + \frac{1}{2}, -z + \frac{1}{2}$; (iii) $x, y + 1, z$; (iv) $-x + \frac{1}{2}, -y - \frac{1}{2}, -z + 1$; (v) $x, -y + 1, z - \frac{1}{2}$.

Table 3

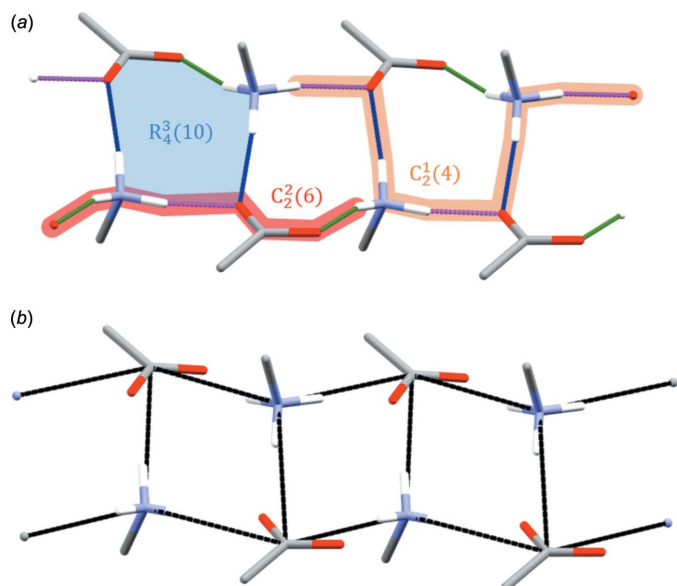
 Hydrogen-bond geometry (Å, °) for **2**.

<i>D</i> —H... <i>A</i>	<i>D</i> —H	H... <i>A</i>	<i>D</i> ... <i>A</i>	<i>D</i> —H... <i>A</i>
O3—H32...O2 ⁱ	0.83 (4)	1.90 (4)	2.728 (4)	175 (4)
O3—H31...O2 ⁱⁱ	0.97 (4)	1.81 (4)	2.771 (4)	169 (3)
N1—H11...O1	0.89 (4)	1.92 (4)	2.791 (4)	168 (4)
N1—H12...O1 ⁱⁱⁱ	0.90 (4)	1.96 (4)	2.805 (4)	157 (4)
N1—H13...O3	0.94 (4)	1.87 (4)	2.809 (4)	170 (3)
C9—H9B...O3 ^{iv}	0.99	2.51	3.196 (4)	126
C15—H15...O2 ⁱ	0.95	2.57	3.412 (4)	147

Symmetry codes: (i) $x, y - 1, z$; (ii) $-x + 1, -y + 1, -z + 1$; (iii) $-x, -y + 1, -z + 1$; (iv) $-x, -y, -z + 1$.

contacts are observed for the phenylacetate molecules in **1** and **2**. Such contacts can come from non-classical C—H...O hydrogen bonds, where the phenylacetate acts as a donor. However, a spike in the fingerprint plots indicating short hydrogen–oxygen distances is only observed for phenylacetate in compound **1** (Fig. 4c) and not in compound **2** (Fig. 4g), implying that C—H...O hydrogen bonds may be more important in **1** than in the hydrate **2**. C...H/H...C intermolecular contacts can arise from close ring contacts of the phenyl rings in the hydrophobic layers, but also from aliphatic C—H... π interactions. An examination of the crystal packings in Figs. 2 and 3 reveals that the phenyl rings are not stacked in a planar, parallel fashion. This is consistent with the absence of C...C intermolecular contacts, which would be expected in such a case (Turner *et al.*, 2017). O...H/H...O and C...H/H...C contacts will be discussed in more detail below.

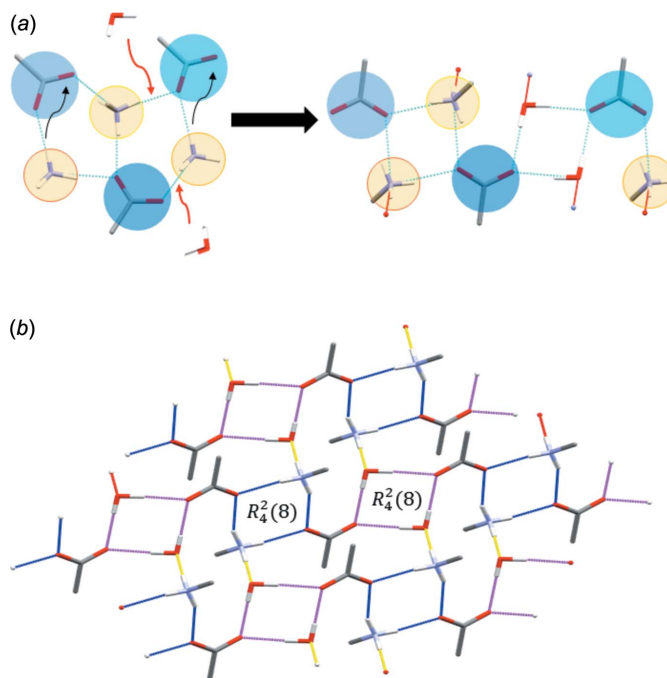
3.2.1. O...H/H...O intermolecular contacts. As mentioned above, O...H/H...O contacts can be attributed mainly to classical and non-classical hydrogen bonds. In compound **1**, intermolecular oxygen–hydrogen contacts amount to about 16 and 26% of the Hirshfeld surface area for the benzylammonium and phenylacetate molecules, respectively. In the hydrate **2**, the values are about 13 and 27%, respectively. The hydrogen-bond parameters for **1** and **2** are summarized in Tables 2 and 3, respectively. In **1**, the classical hydrogen-bonding system involves the benzylammonium molecule as a donor and the phenylacetate molecule as an acceptor for N—H...O hydrogen bonds. In **2**, this system is extended by the presence of the water molecule of crystallization acting as a hydrogen-bond donor and acceptor at the same time. The hydrogen-bonding system in **1** can be described by chain patterns corresponding to a second level graph set


Figure 7

(a) Hydrogen-bonding patterns in **1**. A section of the $C_2^1(4)$ chain pattern is highlighted in orange, and a section of one of the two possible $C_2^2(6)$ chain patterns is highlighted in red. The $R_4^3(10)$ ring pattern is highlighted in blue. Colour code for the hydrogen bonds: N1–H11···O1 green, N1–H12···O2 magenta, N1–H13···O2 blue. (b) Cation–anion ladder motif in **1** formed by the repetition of benzylammonium–phenylacetate pairs. Phenyl rings and CH_2 H atoms are omitted for clarity.

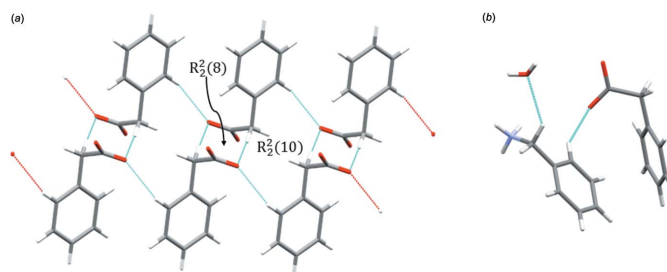
$C_2^2(6)C_2^2(6)C_2^1(4)$ (Bernstein *et al.*, 1995). However, a more obvious feature is the ring structure denoted by a third level pattern $R_4^3(10)$ (Fig. 7a).

The $R_4^3(10)$ ring pattern is a common feature of ammonium carboxylate salts and has been described earlier (Kinbara *et al.*, 1996). Related to this particular ring pattern is an electrostatic ladder motif. Two benzylammonium–phenylacetate (cation–anion) pairs form a dimeric ring, which associates with further cation–anion pairs to form a ladder running along the twofold screw axis of the crystal (Fig. 7b). Such a motif is common in ammonium carboxylate salts (Odendal *et al.*, 2010). Evidently, the presence of crystal water in **2** leads to a change in the hydrogen-bonding system compared to **1**. Going from **1** to **2**, water replaces one of the N–H···O bonds between benzylammonium and phenylacetate. Consequently, the fused $R_4^3(10)$ pattern in **1** is disrupted and two alternating $R_4^2(8)$ patterns bridged by a carboxylate group are formed (Fig. 8a). Those rows are then connected among each other *via* the freed N–H donor group of the benzylammonium molecules and water molecules as acceptors to form a two-dimensional hydrogen-bonding network network (Fig. 8b). Non-classical hydrogen bonds in **1** are formed exclusively between the phenylacetate molecules, forming fused $R_2^2(8)$ and $R_2^2(10)$ ring patterns alternating along the columns around the twofold screw axis along *b*. The hydrogen-bonding system is shown in Fig. 9a. In **2**, the benzylammonium molecule acts as a donor for two discrete non-classical C–H···O hydrogen bonds (Fig. 9b), one with the water molecule of crystallization as acceptor (C9–H9B···O3) and a second one with an oxygen atom of the carboxylate group of phenylacetate (C15–H15···O2).


Figure 8

(a) Transformation of the hydrogen-bonding network in **1** to the network found in **2** by incorporation of crystal water. (b) The two-dimensional hydrogen-bonding network in **2**. Rows of alternating $R_4^2(8)$ motifs (hydrogen bonds highlighted in blue and magenta, respectively) are connected *via* discrete N–H···O hydrogen bonds (highlighted in yellow). Phenyl rings and CH_2 H atoms are omitted for clarity.

3.2.2. C···H/H···C intermolecular contacts. Carbon–hydrogen intermolecular contacts contribute to around one quarter of the Hirshfeld surface areas of the benzylammonium and phenylacetate molecules in both **1** and **2**. As explained above, those contacts are mainly due to close contacts between the phenyl rings in the hydrophobic layers of the crystal packing, but also to (aliphatic) C–H··· π interactions. An automated search using *PLATON* (Spek, 2009) revealed four short ring interactions and one aliphatic C–H··· π interaction in **1** (Fig. 10) and six short ring interactions and one aliphatic C–H··· π interaction in **2** (Fig. 11). The phenyl rings adopt ‘Y’- and ‘T’-shaped edge-to-face arrangements (Martinez & Iverson, 2012) with centroid–centroid distances of 5.019 (1)–5.738 (1) Å in **1** and 5.177 (2)–5.961 (2) Å in **2**. Those


Figure 9

(a) The C–H···O hydrogen-bonding pattern among the phenylacetate molecules in **1** consisting of alternating, fused $R_2^2(8)$ and $R_2^2(10)$ rings. (b) Discrete C–H···O hydrogen bonds in **2**.

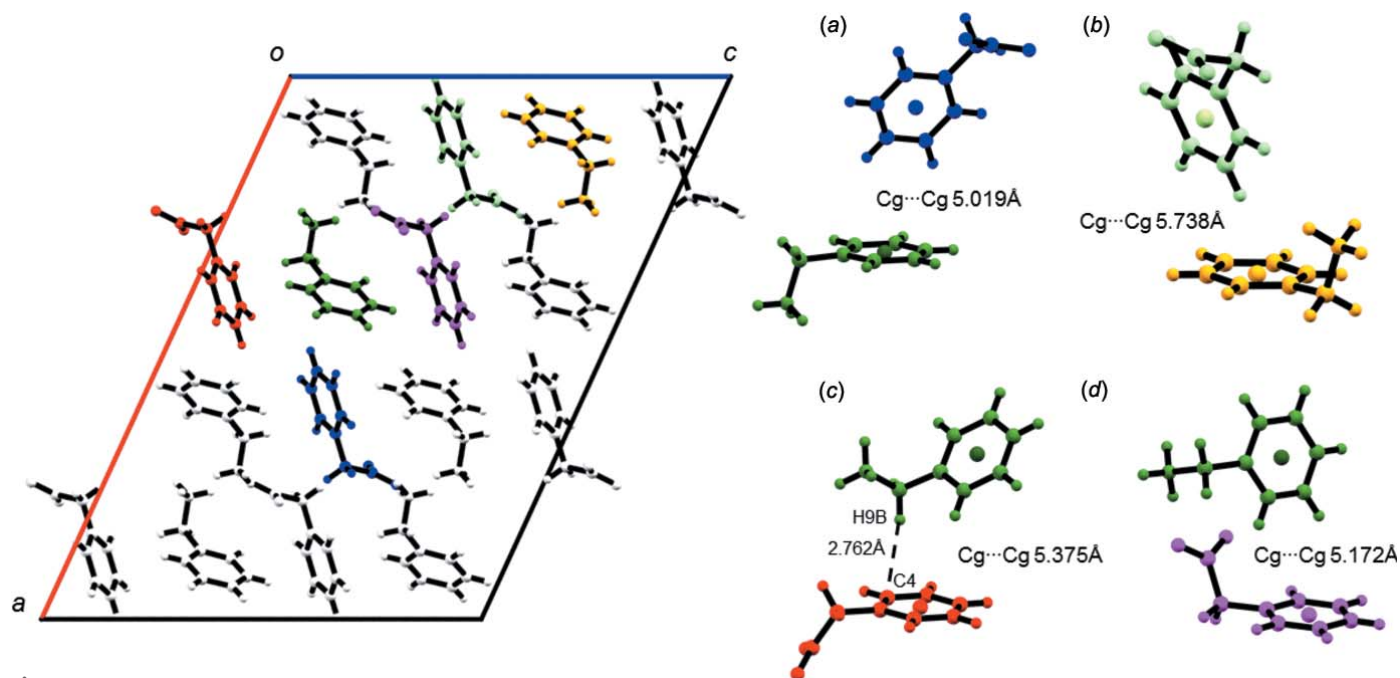


Figure 10
Short ring and aliphatic C—H \cdots π interactions in **1**.

distances are in the same range as the centroid–centroid distance observed in crystalline benzene (Klebe & Diederich, 1993). Close H \cdots C contacts, *i.e.* smaller than the sum of the van der Waals radii (Bondi, 1964; Hu *et al.*, 2014) of the two

elements, are found as part of the aliphatic C—H \cdots π interactions. In **1**, the aliphatic C—H \cdots π interaction is observed between benzylammonium (donor) and phenylacetate (acceptor), with the shortest distance being 2.762 Å between

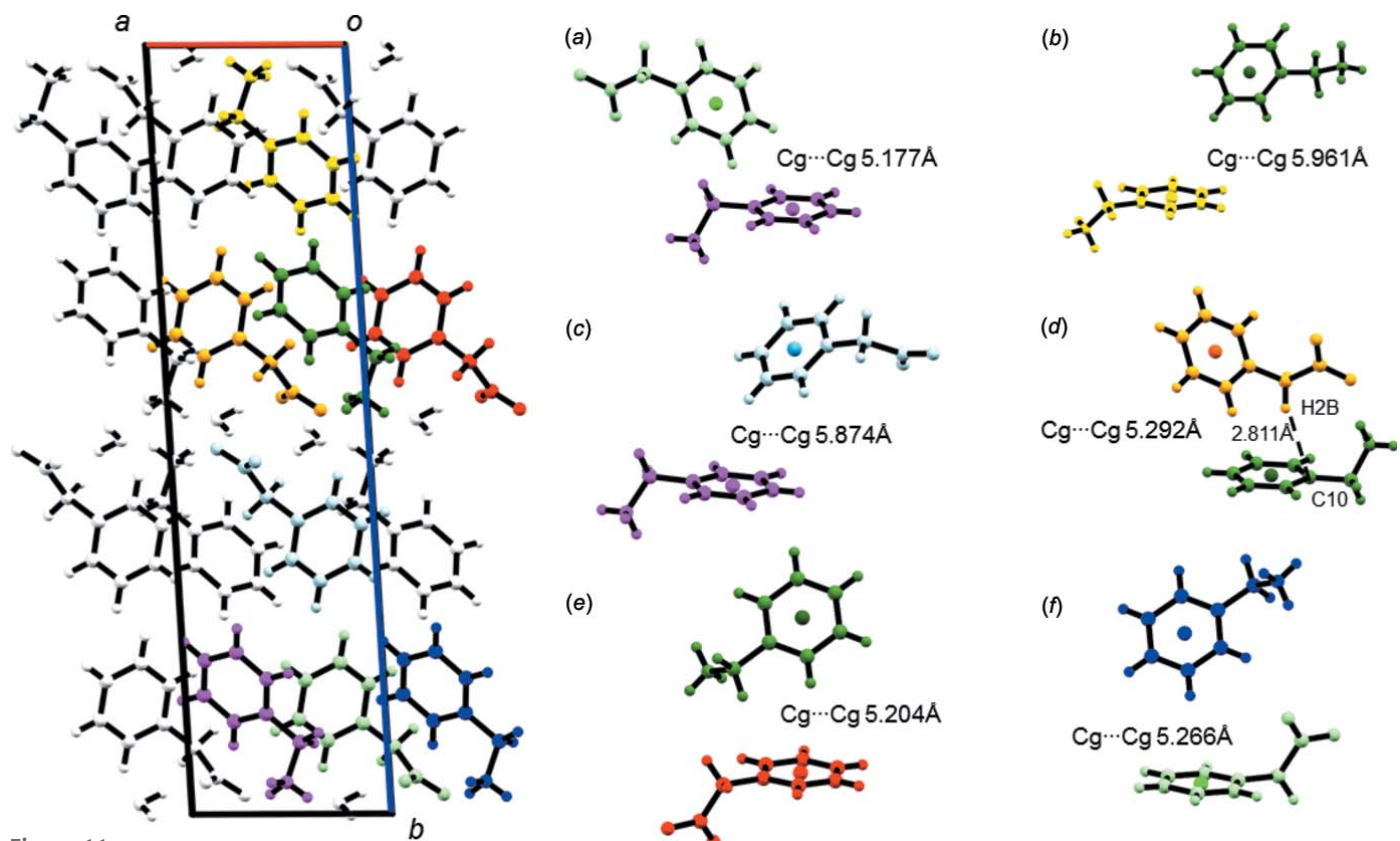


Figure 11
Short ring and aliphatic C—H \cdots π interactions in **2**.

Table 4
Experimental details.

	1	2
Crystal data		
Chemical formula	$C_7H_{10}N^+ \cdot C_8H_7O_2^-$	$C_7H_{10}N^+ \cdot C_8H_7O_2^- \cdot H_2O$
M_r	243.29	261.31
Crystal system, space group	Monoclinic, $C2/c$	Monoclinic, $P2_1/n$
Temperature (K)	100	100
a, b, c (Å)	25.913 (2), 5.9021 (5), 19.0842 (16)	6.8235 (7), 7.8766 (7), 26.364 (2)
β (°)	114.692 (3)	93.218 (3)
V (Å ³)	2651.9 (4)	1414.7 (2)
Z	8	4
Radiation type	Mo $K\alpha$	Mo $K\alpha$
μ (mm ⁻¹)	0.08	0.09
Crystal size (mm)	0.10 × 0.04 × 0.02	0.10 × 0.06 × 0.04
Data collection		
Diffractometer	Bruker D8 Venture TXS	Bruker D8 Venture TXS
Absorption correction	Multi-scan (SADABS; Bruker, 2016)	Multi-scan (SADABS; Bruker, 2016)
T_{min}, T_{max}	0.651, 0.971	0.814, 0.971
No. of measured, independent and observed [$I > 2\sigma(I)$] reflections	14421, 2398, 1800	7319, 2461, 2090
R_{int}	0.092	0.043
$(\sin \theta/\lambda)_{max}$ (Å ⁻¹)	0.602	0.595
Refinement		
$R[F^2 > 2\sigma(F^2)], wR(F^2), S$	0.043, 0.103, 1.03	0.075, 0.170, 1.25
No. of reflections	2398	2461
No. of parameters	175	187
H-atom treatment	H atoms treated by a mixture of independent and constrained refinement	H atoms treated by a mixture of independent and constrained refinement
$\Delta\rho_{max}, \Delta\rho_{min}$ (e Å ⁻³)	0.17, -0.23	0.30, -0.27

Computer programs: APEX3 and SAINT (Bruker, 2015), SHELXT (Sheldrick, 2015a), SHELXL2014/7 (Sheldrick, 2015b), ORTEP-3 for Windows (Farrugia, 2012), Mercury (Macrae *et al.*, 2006), CrystalExplorer17 (Turner *et al.*, 2017), PLATON (Spek, 2009) and RPLUTO (CCDC, 2018).

C9—H9B···C4 (Fig. 10c). In **2**, phenylacetate acts as a donor and benzylammonium as an acceptor for the aliphatic C—H··· π interaction. The closest distance of 2.811 Å is found between C2—H2B···C10 (Fig. 11d). Two more close contacts of the type (C—)H···C can be identified in **2** via the d_{norm} -mapped Hirshfeld surfaces (see H/H' and I/I' in Fig. 6). In the first case, the carbon hydrogen distance C5—H5···C1 (2.812 Å) between two phenylacetate molecules is just below the sum of the van der Waals distances. In the second case, the carbon hydrogen distance C9—H9A···C4 between benzylammonium and phenylacetate is 2.798 Å.

4. Database survey

A structure search on WebCSD (30.11.2018) resulted in 196 hits for structures including benzylammonium and 22 hits for structures including phenylacetate. Structures with packings closely related to those of **1** and **2** containing molecules similar to benzylammonium and phenylacetate can be found in Trivedi & Dastidar (2006; CEKJEI, CEKJIM, CEKJOS), Olmstead *et al.* (2008; HOLDOC), Cai *et al.* (2009; BUDQEX), Das *et al.* (2009; HUKJIH), Mahieux *et al.* (2012; FAHGIG), Tiritiris & Kantlehner (2011; HOLDOC01) and Mossou *et al.* (2014; QQQAUJ03). For a more general view on ammonium carboxylate salts, see Odendal *et al.* (2010) who described the packing motifs in the crystal structures of such

salts, and Kinbara *et al.* (1996) who described the role of hydrogen-bonded networks in the crystal structures of salts of chiral primary amines with achiral carboxylic acids.

5. Synthesis and crystallization

Benzylamine (185701), phenylacetic acid (P16621) and methanol (32213) were obtained from Sigma–Aldrich.

Benzylammonium phenylacetate (**1**) was obtained as follows. 40 mg of phenylacetic acid (0.29 mmol) were dissolved in 1 ml of methanol and 32 μ l of benzylamine (0.29 mmol) were added under gentle stirring. The solvent was then evaporated slowly under ambient conditions to yield colourless crystals of compound **1**.

Benzylammonium phenylacetate hydrate (**2**) was obtained by dissolving 40 mg of phenylacetic acid (0.29 mmol) in 200 μ l of methanol and 32 μ l of benzylamine (0.29 mmol) were added under gentle stirring. The solution was diluted with 1.8 ml of ultra-pure water and evaporated slowly at ambient conditions to yield colourless crystals of compound **2**.

6. Refinement

Crystal data, data collection and structure refinement details are summarized in Table 4. In **1** and **2**, the C-bound hydrogen atoms were positioned with idealized coordinates (C—H =

0.95–0.99 Å) and refined as riding on their parent atoms with $U_{\text{iso}}(\text{H}) = 1.2U_{\text{eq}}(\text{N/O})$. The N-bound hydrogen atoms in **1** were refined freely. In **2**, the coordinates of the N- and O-bound hydrogen atoms were freely refined while the isotropic displacement parameters of the hydrogen atoms were calculated as $U_{\text{iso}}(\text{H}) = 1.2U_{\text{eq}}(\text{N/O})$.

References

- Bernstein, J., Davis, R. E., Shimon, L. & Chang, N.-L. (1995). *Angew. Chem. Int. Ed. Engl.* **34**, 1555–1573.
- Bondi, A. (1964). *J. Phys. Chem.* **68**, 441–451.
- Bruker (2015). *SAINT*. Bruker AXS Inc., Madison, Wisconsin, USA.
- Bruker (2016). *APEX3*. Bruker AXS Inc., Madison, Wisconsin, USA.
- Cai, Y.-J., Dai, X.-B., Liu, L., Li, J. & Li, H.-Y. (2009). *Acta Cryst.* **E65**, o2341.
- CCDC (2018). *RPLUTO*. Cambridge Crystallographic Data Centre, Cambridge, England.
- Das, U. K., Trivedi, D. R., Adarsh, N. N. & Dastidar, P. (2009). *J. Org. Chem.* **74**, 7111–7121.
- Do, T. D., Kincannon, W. M. & Bowers, M. T. (2015). *J. Am. Chem. Soc.* **137**, 10080–10083.
- Eisenberg, D. & Jucker, M. (2012). *Cell*, **148**, 1188–1203.
- Farrugia, L. J. (2012). *J. Appl. Cryst.* **45**, 849–854.
- Gazit, E. (2007). *Chem. Soc. Rev.* **36**, 1263–1269.
- Görlitz, C. H. (2010). *Acta Cryst.* **B66**, 84–93.
- Hu, S.-Z., Zhou, Z.-H., Xie, Z.-X. & Robertson, B. E. (2014). *Z. Krist. Cryst. Mater.* **229**, 517–523.
- Kinbara, K., Hashimoto, Y., Sukegawa, M., Nohira, H. & Saigo, K. (1996). *J. Am. Chem. Soc.* **118**, 3441–3449.
- Klebe, G. & Diederich, F. (1993). *Philos. Trans. R. Soc. London Ser. A*, **345**, 37–48.
- Macrae, C. F., Edgington, P. R., McCabe, P., Pidcock, E., Shields, G. P., Taylor, R., Towler, M. & van de Streek, J. (2006). *J. Appl. Cryst.* **39**, 453–457.
- Mahieux, J., Gonella, S., Sanselme, M. & Coquerel, G. (2012). *CrystEngComm*, **14**, 103–111.
- Manna, M. K., Rasale, D. B. & Das, A. K. (2015). *RSC Adv.* **5**, 90158–90167.
- Martinez, C. R. & Iverson, B. L. (2012). *Chem. Sci.* **3**, 2191–2201.
- McKinnon, J. J., Jayatilaka, D. & Spackman, M. A. (2007). *Chem. Commun.* pp. 3814–3816.
- McManus, J. J., Charbonneau, P., Zaccarelli, E. & Asherie, N. (2016). *Curr. Opin. Colloid Interface Sci.* **22**, 73–79.
- Mossou, E., Teixeira, S. C. M., Mitchell, E. P., Mason, S. A., Adler-Abramovich, L., Gazit, E. & Forsyth, V. T. (2014). *Acta Cryst.* **C70**, 326–331.
- Odendal, J. A., Bruce, J. C., Koch, K. R. & Haynes, D. A. (2010). *CrystEngComm*, **12**, 2398–2408.
- Olmstead, M. M., Franco, J. U. & Pham, D. (2008). Private Communication (Refcode HOLDOC). CCDC, Cambridge, England.
- Ozbas, B., Rajagopal, K., Schneider, J. P. & Pochan, D. J. (2004). *Phys. Rev. Lett.* **93**, 268106.
- Reches, M. & Gazit, E. (2003). *Science*, **300**, 625–627.
- Sheldrick, G. M. (2015a). *Acta Cryst.* **A71**, 3–8.
- Sheldrick, G. M. (2015b). *Acta Cryst.* **C71**, 3–8.
- Spek, A. L. (2009). *Acta Cryst.* **D65**, 148–155.
- Tiritiris, I. & Kantlehner, W. (2011). *Z. Naturforsch. B: Chem. Sci.* **66**, 164–176.
- Trivedi, D. R. & Dastidar, P. (2006). *Chem. Mater.* **18**, 1470–1478.
- Turner, M. J., McKinnon, J. J., Wolff, S. K., Grimwood, D. J., Spackman, P. R., Jayatilaka, D. & Spackman, M. A. (2017). *CrystalExplorer17*. University of Western Australia, Australia.

supporting information

Acta Cryst. (2019). E75, 194-201 [https://doi.org/10.1107/S2056989019000288]

The crystal structures of benzylammonium phenylacetate and its hydrate

David Hess and Peter Mayer

Computing details

For both structures, data collection: *APEX3* (Bruker, 2016); cell refinement: *SAINTE* (Bruker, 2015); data reduction: *SAINTE* (Bruker, 2015); program(s) used to solve structure: *SHELXT* (Sheldrick, 2015a); program(s) used to refine structure: *SHELXL2014/7* (Sheldrick, 2015b); molecular graphics: *ORTEP-3 for Windows* (Farrugia, 2012), *Mercury* (Macrae *et al.*, 2006), *CrystalExplorer17* (Turner *et al.*, 2017); software used to prepare material for publication: *PLATON* (Spek, 2009), *RPLUTO* (CCDC, 2018).

Benzylammonium phenylacetate (1)

Crystal data

$C_7H_{10}N^+ \cdot C_8H_7O_2^-$

$M_r = 243.29$

Monoclinic, *C2/c*

$a = 25.913$ (2) Å

$b = 5.9021$ (5) Å

$c = 19.0842$ (16) Å

$\beta = 114.692$ (3)°

$V = 2651.9$ (4) Å³

$Z = 8$

$F(000) = 1040$

$D_x = 1.219$ Mg m⁻³

Mo *K*α radiation, $\lambda = 0.71073$ Å

Cell parameters from 4302 reflections

$\theta = 3.5$ – 25.4 °

$\mu = 0.08$ mm⁻¹

$T = 100$ K

Block, colourless

$0.10 \times 0.04 \times 0.02$ mm

Data collection

Bruker D8 Venture TXS
diffractometer

Radiation source: rotating anode (TXS), Bruker
TXS

Focusing mirrors monochromator

Detector resolution: 7.4074 pixels mm⁻¹

mix of ϕ and ω scans

Absorption correction: multi-scan
(SADABS; Bruker, 2016)

$T_{\min} = 0.651$, $T_{\max} = 0.971$

14421 measured reflections

2398 independent reflections

1800 reflections with $I > 2\sigma(I)$

$R_{\text{int}} = 0.092$

$\theta_{\max} = 25.4$ °, $\theta_{\min} = 3.3$ °

$h = -30 \rightarrow 30$

$k = -7 \rightarrow 7$

$l = -22 \rightarrow 22$

Refinement

Refinement on F^2

Least-squares matrix: full

$R[F^2 > 2\sigma(F^2)] = 0.043$

$wR(F^2) = 0.103$

$S = 1.03$

2398 reflections

175 parameters

0 restraints

Hydrogen site location: mixed

H atoms treated by a mixture of independent
and constrained refinement

$w = 1/[\sigma^2(F_o^2) + (0.0352P)^2 + 1.6577P]$

where $P = (F_o^2 + 2F_c^2)/3$

$(\Delta/\sigma)_{\max} < 0.001$

$\Delta\rho_{\max} = 0.17$ e Å⁻³

$\Delta\rho_{\min} = -0.22$ e Å⁻³

Special details

Geometry. All esds (except the esd in the dihedral angle between two l.s. planes) are estimated using the full covariance matrix. The cell esds are taken into account individually in the estimation of esds in distances, angles and torsion angles; correlations between esds in cell parameters are only used when they are defined by crystal symmetry. An approximate (isotropic) treatment of cell esds is used for estimating esds involving l.s. planes.

Refinement. C-H: constr N-H: refall

Reflections affected by the beamstop or those of higher order and significant higher F_o^2 than F_c^2 (caused by X-ray mirror) have been omitted in the refinement.

Fractional atomic coordinates and isotropic or equivalent isotropic displacement parameters (\AA^2)

	x	y	z	U_{iso}^*/U_{eq}
O1	0.28279 (5)	-0.35459 (19)	0.41706 (7)	0.0205 (3)
O2	0.24772 (5)	-0.07061 (19)	0.33362 (7)	0.0214 (3)
N1	0.27388 (7)	0.8748 (3)	0.20667 (9)	0.0204 (4)
H11	0.2496 (9)	0.977 (4)	0.1667 (13)	0.040 (6)*
H12	0.2666 (8)	0.714 (4)	0.1867 (12)	0.035 (6)*
H13	0.2661 (10)	0.883 (4)	0.2511 (14)	0.048 (7)*
C1	0.27013 (7)	-0.1506 (3)	0.40169 (10)	0.0169 (4)
C2	0.28113 (7)	0.0118 (3)	0.46855 (10)	0.0190 (4)
H2A	0.2687	0.1656	0.4476	0.023*
H2B	0.2577	-0.0353	0.4958	0.023*
C3	0.34259 (7)	0.0220 (3)	0.52591 (10)	0.0186 (4)
C4	0.36866 (8)	-0.1595 (3)	0.57485 (10)	0.0223 (4)
H4	0.3476	-0.2937	0.5719	0.027*
C5	0.42493 (8)	-0.1460 (3)	0.62768 (11)	0.0266 (4)
H5	0.4421	-0.2705	0.6608	0.032*
C6	0.45623 (8)	0.0480 (3)	0.63248 (11)	0.0307 (5)
H6	0.4948	0.0573	0.6688	0.037*
C7	0.43098 (8)	0.2279 (3)	0.58411 (12)	0.0321 (5)
H7	0.4523	0.3611	0.5869	0.038*
C8	0.37457 (8)	0.2153 (3)	0.53139 (11)	0.0255 (4)
H8	0.3576	0.3407	0.4986	0.031*
C9	0.33454 (8)	0.9379 (3)	0.22888 (11)	0.0273 (5)
H9A	0.3411	1.0948	0.2491	0.033*
H9B	0.3428	0.9326	0.1828	0.033*
C10	0.37371 (7)	0.7794 (3)	0.28918 (10)	0.0220 (4)
C11	0.38860 (8)	0.8179 (3)	0.36684 (11)	0.0281 (5)
H11A	0.3763	0.9525	0.3826	0.034*
C12	0.42124 (8)	0.6622 (4)	0.42177 (11)	0.0354 (5)
H12A	0.4310	0.6898	0.4748	0.042*
C13	0.43957 (9)	0.4672 (4)	0.39950 (13)	0.0375 (5)
H13A	0.4614	0.3592	0.4371	0.045*
C14	0.42609 (8)	0.4292 (3)	0.32244 (13)	0.0357 (5)
H14	0.4394	0.2962	0.3072	0.043*
C15	0.39330 (8)	0.5841 (3)	0.26732 (12)	0.0296 (5)
H15	0.3841	0.5570	0.2144	0.035*

Atomic displacement parameters (\AA^2)

	U^{11}	U^{22}	U^{33}	U^{12}	U^{13}	U^{23}
O1	0.0266 (7)	0.0168 (7)	0.0177 (6)	0.0002 (5)	0.0089 (5)	0.0000 (5)
O2	0.0305 (7)	0.0202 (7)	0.0134 (6)	0.0023 (5)	0.0091 (5)	0.0006 (5)
N1	0.0279 (9)	0.0181 (9)	0.0150 (8)	0.0000 (7)	0.0089 (7)	0.0013 (7)
C1	0.0161 (9)	0.0203 (10)	0.0168 (9)	-0.0024 (7)	0.0093 (7)	-0.0017 (7)
C2	0.0233 (10)	0.0179 (9)	0.0177 (9)	0.0015 (7)	0.0104 (8)	0.0006 (7)
C3	0.0246 (10)	0.0200 (9)	0.0152 (9)	0.0000 (7)	0.0122 (8)	-0.0030 (7)
C4	0.0282 (10)	0.0225 (10)	0.0185 (9)	-0.0023 (8)	0.0119 (8)	-0.0019 (7)
C5	0.0301 (11)	0.0271 (10)	0.0219 (10)	0.0060 (8)	0.0102 (8)	0.0001 (8)
C6	0.0220 (10)	0.0371 (12)	0.0287 (11)	-0.0007 (9)	0.0064 (9)	-0.0081 (9)
C7	0.0290 (11)	0.0275 (11)	0.0393 (12)	-0.0081 (9)	0.0140 (10)	-0.0062 (9)
C8	0.0301 (11)	0.0197 (10)	0.0283 (11)	-0.0014 (8)	0.0138 (9)	-0.0005 (8)
C9	0.0283 (11)	0.0274 (11)	0.0263 (10)	-0.0026 (8)	0.0116 (9)	0.0046 (8)
C10	0.0200 (10)	0.0245 (10)	0.0232 (10)	-0.0038 (7)	0.0105 (8)	0.0019 (8)
C11	0.0233 (10)	0.0377 (12)	0.0260 (11)	-0.0018 (8)	0.0128 (9)	-0.0017 (9)
C12	0.0253 (11)	0.0591 (15)	0.0216 (10)	-0.0011 (10)	0.0097 (9)	0.0073 (10)
C13	0.0219 (11)	0.0422 (13)	0.0402 (13)	0.0006 (9)	0.0051 (10)	0.0176 (10)
C14	0.0222 (11)	0.0292 (11)	0.0481 (14)	0.0001 (8)	0.0073 (10)	-0.0029 (10)
C15	0.0246 (11)	0.0318 (11)	0.0299 (11)	-0.0029 (8)	0.0090 (9)	-0.0037 (9)

Geometric parameters (\AA , $^\circ$)

O1—C1	1.250 (2)	C7—C8	1.388 (3)
O2—C1	1.272 (2)	C7—H7	0.9500
N1—C9	1.494 (2)	C8—H8	0.9500
N1—H11	0.97 (2)	C9—C10	1.501 (3)
N1—H12	1.01 (2)	C9—H9A	0.9900
N1—H13	0.95 (3)	C9—H9B	0.9900
C1—C2	1.525 (2)	C10—C11	1.385 (3)
C2—C3	1.511 (2)	C10—C15	1.392 (3)
C2—H2A	0.9900	C11—C12	1.385 (3)
C2—H2B	0.9900	C11—H11A	0.9500
C3—C8	1.388 (3)	C12—C13	1.378 (3)
C3—C4	1.396 (2)	C12—H12A	0.9500
C4—C5	1.386 (3)	C13—C14	1.381 (3)
C4—H4	0.9500	C13—H13A	0.9500
C5—C6	1.384 (3)	C14—C15	1.385 (3)
C5—H5	0.9500	C14—H14	0.9500
C6—C7	1.379 (3)	C15—H15	0.9500
C6—H6	0.9500		
C9—N1—H11	109.1 (13)	C8—C7—H7	119.8
C9—N1—H12	110.4 (11)	C7—C8—C3	120.88 (18)
H11—N1—H12	109.2 (17)	C7—C8—H8	119.6
C9—N1—H13	109.0 (14)	C3—C8—H8	119.6
H11—N1—H13	111.2 (19)	N1—C9—C10	110.87 (15)

H12—N1—H13	107.9 (17)	N1—C9—H9A	109.5
O1—C1—O2	124.09 (15)	C10—C9—H9A	109.5
O1—C1—C2	118.04 (15)	N1—C9—H9B	109.5
O2—C1—C2	117.86 (15)	C10—C9—H9B	109.5
C3—C2—C1	113.80 (14)	H9A—C9—H9B	108.1
C3—C2—H2A	108.8	C11—C10—C15	118.89 (17)
C1—C2—H2A	108.8	C11—C10—C9	120.98 (17)
C3—C2—H2B	108.8	C15—C10—C9	120.05 (17)
C1—C2—H2B	108.8	C12—C11—C10	120.66 (19)
H2A—C2—H2B	107.7	C12—C11—H11A	119.7
C8—C3—C4	118.27 (17)	C10—C11—H11A	119.7
C8—C3—C2	120.20 (16)	C13—C12—C11	120.06 (19)
C4—C3—C2	121.53 (16)	C13—C12—H12A	120.0
C5—C4—C3	120.69 (17)	C11—C12—H12A	120.0
C5—C4—H4	119.7	C12—C13—C14	119.87 (19)
C3—C4—H4	119.7	C12—C13—H13A	120.1
C6—C5—C4	120.34 (18)	C14—C13—H13A	120.1
C6—C5—H5	119.8	C13—C14—C15	120.2 (2)
C4—C5—H5	119.8	C13—C14—H14	119.9
C7—C6—C5	119.42 (18)	C15—C14—H14	119.9
C7—C6—H6	120.3	C14—C15—C10	120.26 (19)
C5—C6—H6	120.3	C14—C15—H15	119.9
C6—C7—C8	120.39 (18)	C10—C15—H15	119.9
C6—C7—H7	119.8		
O1—C1—C2—C3	59.1 (2)	C2—C3—C8—C7	179.60 (17)
O2—C1—C2—C3	-122.12 (17)	N1—C9—C10—C11	-86.5 (2)
C1—C2—C3—C8	110.26 (18)	N1—C9—C10—C15	90.2 (2)
C1—C2—C3—C4	-70.2 (2)	C15—C10—C11—C12	-1.6 (3)
C8—C3—C4—C5	0.3 (2)	C9—C10—C11—C12	175.07 (17)
C2—C3—C4—C5	-179.29 (16)	C10—C11—C12—C13	0.4 (3)
C3—C4—C5—C6	-0.3 (3)	C11—C12—C13—C14	1.0 (3)
C4—C5—C6—C7	-0.1 (3)	C12—C13—C14—C15	-1.3 (3)
C5—C6—C7—C8	0.4 (3)	C13—C14—C15—C10	0.0 (3)
C6—C7—C8—C3	-0.4 (3)	C11—C10—C15—C14	1.4 (3)
C4—C3—C8—C7	0.0 (3)	C9—C10—C15—C14	-175.34 (18)

Hydrogen-bond geometry (Å, °)

Cg1 is the centroid of the C3—C8 ring.

<i>D</i> —H··· <i>A</i>	<i>D</i> —H	H··· <i>A</i>	<i>D</i> ··· <i>A</i>	<i>D</i> —H··· <i>A</i>
N1—H11···O1 ⁱ	0.97 (2)	1.77 (2)	2.7177 (19)	165 (2)
N1—H12···O2 ⁱⁱ	1.01 (2)	1.73 (2)	2.7306 (19)	170.1 (18)
N1—H13···O2 ⁱⁱⁱ	0.95 (3)	1.85 (3)	2.7938 (19)	174 (2)
C2—H2B···O1 ^{iv}	0.99	2.40	3.375 (2)	169

C8—H8...O1 ⁱⁱⁱ	0.95	2.63	3.539 (2)	161
C9—H9...Cg1 ^v	0.95	2.92	3.877 (2)	163

Symmetry codes: (i) $-x+1/2, y+3/2, -z+1/2$; (ii) $-x+1/2, y+1/2, -z+1/2$; (iii) $x, y+1, z$; (iv) $-x+1/2, -y-1/2, -z+1$; (v) $x, -y+1, z-1/2$.

Benzylammonium phenylacetate (2)

Crystal data

$C_7H_{10}N^+ \cdot C_8H_7O_2^- \cdot H_2O$

$M_r = 261.31$

Monoclinic, $P2_1/n$

$a = 6.8235$ (7) Å

$b = 7.8766$ (7) Å

$c = 26.364$ (2) Å

$\beta = 93.218$ (3)°

$V = 1414.7$ (2) Å³

$Z = 4$

$F(000) = 560$

$D_x = 1.227$ Mg m⁻³

Mo $K\alpha$ radiation, $\lambda = 0.71073$ Å

Cell parameters from 4619 reflections

$\theta = 2.7$ – 25.0 °

$\mu = 0.09$ mm⁻¹

$T = 100$ K

Block, colourless

$0.10 \times 0.06 \times 0.04$ mm

Data collection

Bruker D8 Venture TXS

diffractometer

Radiation source: rotating anode (TXS), Bruker TXS

Focusing mirrors monochromator

Detector resolution: 7.4074 pixels mm⁻¹

mix of ϕ and ω scans

Absorption correction: multi-scan (SADABS; Bruker, 2016)

$T_{\min} = 0.814, T_{\max} = 0.971$

7319 measured reflections

2461 independent reflections

2090 reflections with $I > 2\sigma(I)$

$R_{\text{int}} = 0.043$

$\theta_{\max} = 25.0$ °, $\theta_{\min} = 3.5$ °

$h = -7 \rightarrow 7$

$k = -9 \rightarrow 8$

$l = -31 \rightarrow 27$

Refinement

Refinement on F^2

Least-squares matrix: full

$R[F^2 > 2\sigma(F^2)] = 0.075$

$wR(F^2) = 0.170$

$S = 1.25$

2461 reflections

187 parameters

0 restraints

Hydrogen site location: mixed

H atoms treated by a mixture of independent and constrained refinement

$w = 1/[\sigma^2(F_o^2) + 3.8665P]$

where $P = (F_o^2 + 2F_c^2)/3$

$(\Delta/\sigma)_{\max} < 0.001$

$\Delta\rho_{\max} = 0.30$ e Å⁻³

$\Delta\rho_{\min} = -0.27$ e Å⁻³

Special details

Geometry. All esds (except the esd in the dihedral angle between two l.s. planes) are estimated using the full covariance matrix. The cell esds are taken into account individually in the estimation of esds in distances, angles and torsion angles; correlations between esds in cell parameters are only used when they are defined by crystal symmetry. An approximate (isotropic) treatment of cell esds is used for estimating esds involving l.s. planes.

Refinement. C-H constr N-H and O-H: refxyz

Fractional atomic coordinates and isotropic or equivalent isotropic displacement parameters (Å²)

	<i>x</i>	<i>y</i>	<i>z</i>	$U_{\text{iso}}^*/U_{\text{eq}}$
O1	0.2350 (3)	0.5687 (3)	0.47484 (9)	0.0213 (6)
O2	0.4238 (4)	0.7897 (3)	0.45801 (10)	0.0245 (6)
O3	0.2403 (4)	0.0283 (3)	0.51346 (10)	0.0230 (6)
H32	0.296 (6)	-0.048 (6)	0.4981 (15)	0.028*
H31	0.355 (6)	0.089 (5)	0.5279 (15)	0.028*

N1	0.0153 (5)	0.2727 (4)	0.45885 (12)	0.0205 (7)
H11	0.091 (6)	0.364 (5)	0.4595 (14)	0.025*
H12	-0.084 (6)	0.296 (5)	0.4786 (15)	0.025*
H13	0.101 (6)	0.191 (5)	0.4742 (14)	0.025*
C1	0.3709 (5)	0.6394 (4)	0.45153 (13)	0.0174 (7)
C2	0.4705 (5)	0.5289 (5)	0.41280 (13)	0.0213 (8)
H2A	0.5366	0.4332	0.4311	0.026*
H2B	0.3676	0.4802	0.3892	0.026*
C3	0.6199 (5)	0.6182 (4)	0.38174 (13)	0.0190 (8)
C4	0.8017 (5)	0.6658 (4)	0.40418 (14)	0.0210 (8)
H4	0.8333	0.6385	0.4388	0.025*
C5	0.9377 (5)	0.7532 (5)	0.37627 (14)	0.0236 (8)
H5	1.0604	0.7860	0.3921	0.028*
C6	0.8942 (6)	0.7920 (5)	0.32577 (14)	0.0272 (9)
H6	0.9862	0.8522	0.3069	0.033*
C7	0.7154 (6)	0.7424 (5)	0.30294 (14)	0.0280 (9)
H7	0.6851	0.7674	0.2681	0.034*
C8	0.5802 (5)	0.6560 (5)	0.33093 (14)	0.0239 (8)
H8	0.4583	0.6223	0.3149	0.029*
C9	-0.0635 (5)	0.2271 (5)	0.40676 (13)	0.0226 (8)
H9A	-0.1605	0.3136	0.3947	0.027*
H9B	-0.1320	0.1165	0.4080	0.027*
C10	0.0974 (5)	0.2156 (4)	0.36952 (13)	0.0198 (8)
C11	0.0829 (6)	0.3063 (5)	0.32460 (14)	0.0253 (8)
H11A	-0.0272	0.3778	0.3174	0.030*
C12	0.2285 (6)	0.2938 (5)	0.28976 (14)	0.0330 (10)
H12A	0.2175	0.3567	0.2590	0.040*
C13	0.3896 (6)	0.1892 (5)	0.30013 (15)	0.0315 (10)
H13A	0.4887	0.1800	0.2764	0.038*
C14	0.4056 (6)	0.0986 (5)	0.34496 (14)	0.0273 (9)
H14	0.5164	0.0278	0.3521	0.033*
C15	0.2608 (5)	0.1105 (4)	0.37956 (14)	0.0222 (8)
H15	0.2722	0.0472	0.4102	0.027*

Atomic displacement parameters (\AA^2)

	U^{11}	U^{22}	U^{33}	U^{12}	U^{13}	U^{23}
O1	0.0211 (13)	0.0190 (13)	0.0243 (13)	-0.0042 (10)	0.0064 (10)	-0.0027 (11)
O2	0.0237 (14)	0.0181 (13)	0.0321 (15)	-0.0035 (11)	0.0068 (10)	-0.0066 (12)
O3	0.0200 (14)	0.0212 (14)	0.0279 (15)	-0.0001 (11)	0.0032 (10)	-0.0061 (12)
N1	0.0205 (16)	0.0160 (16)	0.0254 (17)	-0.0024 (13)	0.0050 (13)	-0.0044 (14)
C1	0.0122 (17)	0.0197 (18)	0.0201 (18)	-0.0014 (14)	-0.0011 (13)	-0.0014 (15)
C2	0.0248 (19)	0.0182 (18)	0.0213 (19)	-0.0018 (15)	0.0051 (14)	-0.0035 (15)
C3	0.0200 (18)	0.0145 (17)	0.0229 (19)	0.0030 (14)	0.0052 (14)	-0.0045 (15)
C4	0.0241 (19)	0.0192 (18)	0.0197 (18)	-0.0003 (15)	0.0020 (14)	-0.0012 (15)
C5	0.0208 (18)	0.0188 (19)	0.031 (2)	0.0001 (15)	0.0034 (15)	-0.0036 (16)
C6	0.029 (2)	0.025 (2)	0.029 (2)	-0.0042 (17)	0.0114 (16)	-0.0020 (17)
C7	0.032 (2)	0.031 (2)	0.0213 (19)	0.0023 (18)	0.0045 (15)	0.0034 (17)

C8	0.0175 (18)	0.030 (2)	0.024 (2)	-0.0029 (16)	0.0018 (14)	-0.0048 (17)
C9	0.0228 (19)	0.0222 (19)	0.0229 (19)	-0.0023 (15)	0.0019 (14)	-0.0030 (16)
C10	0.0242 (19)	0.0157 (17)	0.0195 (18)	-0.0086 (15)	0.0026 (14)	-0.0055 (15)
C11	0.030 (2)	0.025 (2)	0.0211 (19)	-0.0030 (16)	-0.0035 (15)	-0.0024 (16)
C12	0.046 (3)	0.035 (2)	0.0176 (19)	-0.011 (2)	0.0033 (17)	0.0000 (18)
C13	0.029 (2)	0.039 (2)	0.028 (2)	-0.0050 (18)	0.0110 (16)	-0.0072 (19)
C14	0.028 (2)	0.025 (2)	0.029 (2)	-0.0025 (16)	0.0054 (16)	-0.0052 (17)
C15	0.029 (2)	0.0142 (17)	0.0236 (19)	-0.0006 (15)	0.0046 (15)	-0.0017 (15)

Geometric parameters (Å, °)

O1—C1	1.270 (4)	C6—H6	0.9500
O2—C1	1.247 (4)	C7—C8	1.391 (5)
O3—H32	0.83 (4)	C7—H7	0.9500
O3—H31	0.97 (4)	C8—H8	0.9500
N1—C9	1.490 (4)	C9—C10	1.516 (5)
N1—H11	0.89 (4)	C9—H9A	0.9900
N1—H12	0.90 (4)	C9—H9B	0.9900
N1—H13	0.94 (4)	C10—C11	1.382 (5)
C1—C2	1.529 (5)	C10—C15	1.402 (5)
C2—C3	1.516 (5)	C11—C12	1.394 (5)
C2—H2A	0.9900	C11—H11A	0.9500
C2—H2B	0.9900	C12—C13	1.389 (6)
C3—C8	1.384 (5)	C12—H12A	0.9500
C3—C4	1.395 (5)	C13—C14	1.380 (6)
C4—C5	1.398 (5)	C13—H13A	0.9500
C4—H4	0.9500	C14—C15	1.385 (5)
C5—C6	1.382 (5)	C14—H14	0.9500
C5—H5	0.9500	C15—H15	0.9500
C6—C7	1.386 (5)		
H32—O3—H31	100 (4)	C6—C7—H7	120.0
C9—N1—H11	113 (3)	C8—C7—H7	120.0
C9—N1—H12	110 (2)	C3—C8—C7	121.3 (3)
H11—N1—H12	106 (4)	C3—C8—H8	119.4
C9—N1—H13	114 (2)	C7—C8—H8	119.4
H11—N1—H13	102 (3)	N1—C9—C10	112.0 (3)
H12—N1—H13	111 (3)	N1—C9—H9A	109.2
O2—C1—O1	124.3 (3)	C10—C9—H9A	109.2
O2—C1—C2	119.7 (3)	N1—C9—H9B	109.2
O1—C1—C2	116.0 (3)	C10—C9—H9B	109.2
C3—C2—C1	115.7 (3)	H9A—C9—H9B	107.9
C3—C2—H2A	108.3	C11—C10—C15	119.0 (3)
C1—C2—H2A	108.3	C11—C10—C9	120.3 (3)
C3—C2—H2B	108.3	C15—C10—C9	120.7 (3)
C1—C2—H2B	108.3	C10—C11—C12	120.6 (4)
H2A—C2—H2B	107.4	C10—C11—H11A	119.7
C8—C3—C4	118.3 (3)	C12—C11—H11A	119.7

C8—C3—C2	121.5 (3)	C13—C12—C11	119.9 (4)
C4—C3—C2	120.3 (3)	C13—C12—H12A	120.1
C3—C4—C5	120.7 (3)	C11—C12—H12A	120.1
C3—C4—H4	119.7	C14—C13—C12	119.9 (4)
C5—C4—H4	119.7	C14—C13—H13A	120.0
C6—C5—C4	120.2 (3)	C12—C13—H13A	120.0
C6—C5—H5	119.9	C13—C14—C15	120.3 (4)
C4—C5—H5	119.9	C13—C14—H14	119.9
C5—C6—C7	119.5 (3)	C15—C14—H14	119.9
C5—C6—H6	120.3	C14—C15—C10	120.3 (3)
C7—C6—H6	120.3	C14—C15—H15	119.8
C6—C7—C8	120.1 (3)	C10—C15—H15	119.8
O2—C1—C2—C3	-4.5 (5)	C6—C7—C8—C3	0.2 (6)
O1—C1—C2—C3	174.7 (3)	N1—C9—C10—C11	-126.9 (4)
C1—C2—C3—C8	-107.2 (4)	N1—C9—C10—C15	54.4 (4)
C1—C2—C3—C4	72.2 (4)	C15—C10—C11—C12	0.0 (5)
C8—C3—C4—C5	1.6 (5)	C9—C10—C11—C12	-178.8 (3)
C2—C3—C4—C5	-177.8 (3)	C10—C11—C12—C13	0.1 (6)
C3—C4—C5—C6	-0.7 (5)	C11—C12—C13—C14	-0.3 (6)
C4—C5—C6—C7	-0.5 (6)	C12—C13—C14—C15	0.5 (6)
C5—C6—C7—C8	0.8 (6)	C13—C14—C15—C10	-0.5 (6)
C4—C3—C8—C7	-1.4 (5)	C11—C10—C15—C14	0.2 (5)
C2—C3—C8—C7	178.1 (3)	C9—C10—C15—C14	178.9 (3)

Hydrogen-bond geometry (Å, °)

<i>D</i> —H... <i>A</i>	<i>D</i> —H	H... <i>A</i>	<i>D</i> ... <i>A</i>	<i>D</i> —H... <i>A</i>
O3—H32...O2 ⁱ	0.83 (4)	1.90 (4)	2.728 (4)	175 (4)
O3—H31...O2 ⁱⁱ	0.97 (4)	1.81 (4)	2.771 (4)	169 (3)
N1—H11...O1	0.89 (4)	1.92 (4)	2.791 (4)	168 (4)
N1—H12...O1 ⁱⁱⁱ	0.90 (4)	1.96 (4)	2.805 (4)	157 (4)
N1—H13...O3	0.94 (4)	1.87 (4)	2.809 (4)	170 (3)
C9—H9B...O3 ^{iv}	0.99	2.51	3.196 (4)	126
C15—H15...O2 ⁱ	0.95	2.57	3.412 (4)	147

Symmetry codes: (i) $x, y-1, z$; (ii) $-x+1, -y+1, -z+1$; (iii) $-x, -y+1, -z+1$; (iv) $-x, -y, -z+1$.